Research Article

Journal of Molecular Recognition

Received: 11 February 2008, Revised: 31 March 2008, Accepted: 4 April 2008, Published online in Wiley InterScience: 21 May 2008

(www.interscience.wiley.com) DOI:10.1002/jmr.894

Online optimization of surface plasmon resonance-based biosensor experiments for improved throughput and confidence

Gregory De Crescenzo[a]*, Lyne Woodward[a] and Bala Srinivasan[a]

The emergence of surface plasmon resonance-based optical biosensors has facilitated the identification of kinetic parameters for various macromolecular interactions. Normally, these parameters are determined from experiments with arbitrarily chosen periods of macromolecule and buffer injections, and varying macromolecule concentrations. Since the choice of these variables is arbitrary, such experiments may not provide the required confidence in identified kinetic parameters expressed in terms of standard errors. In this work, an iterative optimization approach is used to determine the above-mentioned variables so as to reduce the experimentation time, while treating the required standard errors as constraints. It is shown using multiple experimental and simulated data that the desired confidence can be reached with much shorter experiments than those generally performed by biosensor users. Copyright © 2008 John Wiley & Sons, Ltd.

Keywords: surface plasmon resonance (SPR); biosensor; online optimization; kinetics

INTRODUCTION

Identification of thermodynamic and kinetic parameters related to macromolecular interactions are key issues in many fields of biosciences including structural biology, protein engineering, and rational drug design. For example, a thermodynamic characterization of macromolecular complexes provides information that can be advantageously correlated to X-ray or NMR results in order to identify critical residues or domains for the interactions under study (Kozlov *et al*., 2004; De Crescenzo *et al*., 2006) as well as to provide guidance for the identification of putative natural binders (Lim *et al*., 2006) or for the rational design of *de novo* inhibitors (De Crescenzo *et al*., 2004; Sarrazin *et al*., 2005).

In many cases, however, characterizing the kinetics of a macromolecular interaction is more relevant than its thermodynamic depiction. That is, kinetic characterization is better suited for the understanding of molecular functions since most biological processes do not reach equilibrium (Krogsgaard *et al*., 2003; Wiley *et al*., 2003) and since differences in kinetics may lead to marked differences in biological outcomes, while compensating each other to result in similar affinities (Lenferink *et al*., 2000). The determination of kinetic parameters is also key for quality assessment of recombinant proteins used as therapeutics (DiGiacomo *et al*., 2004; Kikuchi *et al*., 2005).

In essence, kinetic constant determination implies real-time measurements, for which surface plasmon resonance (SPR)-based biosensors have emerged as a new (Fägerstam *et al*., 1990) and versatile (Rich and Myszka, 2006) approach during the last two decades. Among the SPR biosensors commercially available (Rich and Myszka, 2000; McDonnell, 2001), the Biacore™ instruments (BIACORE Inc.) are widely recognized to provide state-of-the-art technology for kinetic characterization, as one can judge by the increasing numbers of scientific reports in which these biosensors are used. Such a success can be mainly attributed to (i) the relative ease of data collection since detection does not necessitate any labeling; (ii) the great diversity of surfaces and chemistry protocols developed for immobilizing one of the species under study at the surface of the biosensor chips; and (iii) the detection limit of the instruments that allows to monitor interactions involving small molecular weight compounds (MW $<$ 200 Da) to large species whose molecular weights exceed 100 kDa in addition to determining kinetic rates almost spanning the entire range of the biological spectrum (Myszka *et al*., 1998).

In the Biacore™ optical biosensors, SPR is applied to detect the refractive index changes that occur when a soluble species, being continuously delivered at a specific concentration through the biosensor flow cell, interacts with its binding partner that had been previously immobilized at the biosensor surface. This signal that is recorded in real time is proportional to the mass accumulation resulting from complex formation at the biosensor surface and is reported in arbitrary resonance units (RU). Subsequent buffer injection results in the dissociation of previously formed complexes that can also be followed in real time. If necessary, injection of a regeneration solution is performed in order to promote complete complex dissociation (i.e., by varying the pH, salt and/or detergent concentrations). This sequence of events (complex formation, dissociation, and regeneration steps) is called a sensorgram in the Biacore™

* *Correspondence to: G. De Crescenzo, Bio-P2 unit, Department of Chemical Engineering, École Polytechnique de Montréal, P. O. Box 6079, Centre-ville Station, Montréal, Québec, Canada H3C 3A7.*
E-mail: gregory.decrescenzo@polymtl.ca

a *G. De Crescenzo, L. Woodward, B. Srinivasan*
Department of Chemical Engineering, École Polytechnique de Montréal, P. O. Box 6079, Centre-ville Station, Montréal, Québec, Canada H3C 3A7

Journal of Molecular Recognition

terminology. This cycle can be repeated by varying the temperature, the concentration of the molecule to be injected as well as the duration and flow rate at which the injection and dissociation phases are performed. Assuming that the regeneration step does not affect the biophysical properties of the immobilized species, this leads to the recording of a set of sensorgrams that depicts the interactions between the soluble species and its binding partner (attached to the sensor chip surface).

The rapid dissemination of the SPR technology has been soon accompanied by skepticism about the validity of kinetic and thermodynamic parameters derived from sensorgram analysis. Among all the criticisms raised, the large majority of them relied on the possible appearance of artifacts resulting from the use of surfaces on which immobilization of one of the macromolecules under study is performed. For example, in the case of proteins, standard protocols based on the availability of amine groups present on lysine side chain and at the N-terminus of proteins may result in obtaining various protein populations characterized by different kinetics when interacting with their binding partner (O'Shannessy and Winzor, 1996). Furthermore, the coupling itself, even if homogenous, results in a loss of rotational freedom for the surface-bound species that, in turn, may cause a significant deviation of its kinetics of interactions when compared to true solution-based measurements. Also, monitoring the interactions between surface-bound and soluble macromolecules implies that, prior to interacting, the soluble species has to diffuse from the bulk flow to the surface vicinity. If the diffusion kinetic is slow as compared to the kinetics of interactions, the sensorgram profile will be affected (Myszka *et al*., 1998). In addition, interactions between injected binding partners and the three-dimensional matrix of the biosensor chip surface may occur and should thus be taken into account or discarded (Myszka, 1997; Morton and Myszka, 1998). Contrary to the above arguments, it was demonstrated that thermodynamic and kinetic constants derived from Biacore™ experiments matched those acquired by other solution-based biophysical methods such as isothermal titration calorimetry and stopped-flow fluorescence (Day *et al*., 2002). Such a consensus was made possible thanks to the development of experimental strategies aiming at eliminating the above-mentioned artifacts (e.g., reducing immobilized species levels, adopting coupling strategies for orienting macromolecule capture, working at high flow rate, performing double referencing, etc., see Rich and Myszka, 2000 and references therein) in combination with the implementation of numerical approaches to analyze biosensor data in a rigorous and robust fashion (Fisher *et al*., 1994; Myszka and Morton, 1998; De Crescenzo *et al*., 2000; Ben Khalifa *et al*., 2001; Svitel *et al*., 2003).

Of interest, the latest SPR-based biosensor developments have been directed to provide researchers with tools combining the flexibility and information-rich measurements of SPR systems to the high-throughput capacity of standard *in vitro* assays such as ELISA or *in vitro* cell assays. Hence, a new generation of biosensors allowing for testing of one sample against up to 400 targets, or testing multiple samples onto multiple surfaces in parallel has come into place (Rich and Myszka, 2007). These new devices have already been reported to be extremely useful in the new field of proteomics. However, as outlined by Rich and Myszka, in most cases quantity is still detrimental to quality so far, as most of the multi-array systems available now do not permit to reach the same in-depth kinetic analysis as low throughput systems.

One of the key aspects in kinetic parameter estimation is the level of confidence that can be attributed to the estimated parameters. In this paper, it is measured using the standard error. The value of the standard error defined as in Önell and Andersson (2005) is a function of several factors: (i) the noise level in the measurements; (ii) the number of data points; and (iii) the experimental plan that is utilized (Ober and Ward, 1999). The noise level in Biacore™ instruments is already quite low and the current work is not addressed to the instrumentation design that could potentially reduce it or increase the level of detection achieved with the current instruments. The standard error is inversely proportional to the square root of the number of data points, and thus, better confidence can be obtained by having more data or multiple experiments. In this work, the experiments were performed in duplicate (unless indicated) and a high sampling rate (10 Hz) was considered.

However, the third aspect, that is, the relationship between the standard error and the experimental plan will be investigated in detail in this work. That is, assuming that the interactions under study are Langmuirian, if the association kinetic constant is fairly rapid and if a high concentration of the analyte is used, then the response would reach saturation fairly quickly, thereby providing very few experimental points in the portion of the sensorgram that is transient (i.e., prior to plateau) for the determination of the kinetic constants. So, intuitively, the confidence on this parameter would be low. On the other hand, if a low concentration of analyte is used, the transient portion of the recorded signal would indeed be longer thereby leading to a better confidence on the parameters. Turning to the dissociation constant, the higher the value of the signal and the higher the decrease in the recorded signal during the dissociation period, the better would be the confidence.

These considerations lead to two important conclusions: (i) the best operating condition depends on the values of kinetic constants, for example, a certain experiment is optimal for rapid association—rapid dissociation scenario, while a completely different experiment is needed to provide optimal results for the rapid association—slow dissociation scenario; (ii) one typically needs multiple experiments, for example, in the rapid association—low dissociation scenario, as discussed earlier, one needs a low concentration of the analyte to be injected to get a longer transient response for a good determination of the association constant, while a higher analyte concentration is needed for improving the confidence in the dissociation constant.

Typically, Biacore users report globally analyzed data corresponding to 5–10 different injections with varying analyte concentrations over as wide a range of concentrations as possible. However, recently, Önell and Andersson (2005) showed that typically two experiments are sufficient to get the same level of confidence as that of the experiments traditionally performed. The key issue is still the choice of two appropriate out of 5–10 experiments. This choice thus depends on the kinetic constants and, up to now, could be performed *a posteriori* taking into account preliminary data sets and quantities of material available. This work extends the study of Önell and Andersson (2005), by providing a constructive method to choose the minimum number of experiments *online* using a numerical optimization framework. In addition, the duration for association and dissociation are considered to be variable.

In the present study, we demonstrate that a careful planning of SPR-based biosensor experiments, using online numerical optimization based on parameter estimation and confidence

evaluation, does indeed result in a significant reduction of experiment time and material consumption with level of confidence on estimated parameters identical to those derived from classical experiments. Our results further suggest that such an experimental planning can be performed online in a fully automated fashion when biological systems under study are adequately described by a simple Langmuirian model. The implementation of our approach may thus pave the way for increased throughput of current SPR instruments without any loss on kinetic paramater confidence.

Theory

Modeling of the interaction

The system under study corresponds to continuous injections of protein (the analyte, denoted A) at defined concentrations, over a Biacore™ surface on which its binding partner (the ligand, denoted B) had been previously coupled. Their interaction results in the formation of a non-covalent complex AB that can, in turn, dissociate when the protein solution is replaced by a continuous injection of buffer. Assuming that the interaction is Langmuirian, it can then be depicted by the following scheme:

$$A + B \underset{k_d}{\overset{k_a}{\rightleftharpoons}} AB$$

where k_a and k_d are the association and dissociation rate constants of the interaction expressed in $M^{-1}s^{-1}$ and s^{-1}, respectively. The above interaction is followed by monitoring the resulting product AB (in RU). The following set of equations can thus be derived from the previous scheme in order to depict the interactions:

$$\begin{aligned} &\dot{R}_{AB} = k_a C_A (R_{max} - R_{AB}) - k_d R_{AB},\ R_{AB}(0) = 0 \\ &R = \begin{cases} R_{AB} + R_A, & \text{if} \quad C_A \neq 0 \\ R_{AB}, & \text{if} \quad C_A = 0 \end{cases} \end{aligned} \tag{1}$$

where C_A is the concentration of free analyte A (in M), R_{max} the maximal amount of analyte that can specifically bind to the surface (in RU), R_{AB} the amount of AB complex (in RU), R_A is a correction factor (in RU) that is added to take into account refractive index artifacts that are often observed at the beginning of each phase of a sensorgram even after control correction of the signal. R is the resulting recorded signal in RU.

Parameter identification problem

In order to identify the parameters k_a and k_d, a series of experiments with varying concentrations of analyte A (C_A) are performed. Each experiment consists of an on-period (analyte injection) t_{on} and an off-period (buffer injection) t_{off}, both expressed in seconds, during which signal is acquired at a sampling frequency of 10 Hz. From the experimental data, the following least-squared identification algorithm is utilized to compute the required parameters:

$$\min_{k_a, k_d, R_{max}, R_A^i} \sum_{i=1}^{N} \frac{1}{T^i} \sum_{j=0}^{M^i} \left(R^i_{meas}(j) - R^i_{pred}(j)\right)^2$$

where N is the number of experiments, $T^i = t^i_{on} + t^i_{off}$, the duration of the ith experiment, M^i the number of data points in sensogram i, $R^i_{meas}(t)$ the measurements, and $R^i_{pred}(t)$ the prediction from the model presented in Equation (1). Note that the parameters R_{max} and R^i_A the resonance signal of analyte A in the ith experiment should also be included in the identification procedure. Also, the integral form is used for parameter estimation, since it is less prone to measurement errors and more easily generalized.

Confidence and standard error

One of the important aspects while performing identification is the confidence one has in the parameters. This primarily depends on the measurement noise, the number of measurements, and also on the experimental planning. There are various ways of expressing the confidence and the one widely used in this domain is the standard error. The standard error ξ_j in parameter j can be expressed as follows (Önell and Andersson, 2005):

$$\xi_j = \rho\sigma\sqrt{(\boldsymbol{H}^{-1})_{jj}}$$

where ρ is a proportionality constant based on the Student's F distribution, the number of points used, and the level of confidence that is requested, σ the standard deviation of the measurement noise, and $(H^{-1})_{jj}$, the jth diagonal element of the inverse of the Hessian matrix H, which will be discussed in detail next. The Hessian matrix is given by

$$\boldsymbol{H} = \sum_{i=1}^{N} \frac{1}{T^i} \sum_{j=1}^{M^i} \left(\frac{\partial R^i_{pred}(j)}{\partial \theta}\right)^{\mathrm{T}} \left(\frac{\partial R^i_{pred}(j)}{\partial \theta}\right), \quad \theta = \begin{bmatrix} k_a \\ k_d \\ R_{max} \\ R^i_A \end{bmatrix} \tag{2}$$

Calculation of the Hessian: For calculating the standard error, it can be seen that obtaining the Hessian is crucial. The calculation of the Hessian involves solving the following differential equations along with the system Equation (1):

$$\frac{\partial R_{pred}}{\partial k_a} \equiv x_1, \quad \frac{\partial R_{pred}}{\partial k_d} \equiv x_2, \quad \frac{\partial R_{pred}}{\partial R_{max}} \equiv x_3, \quad \frac{\partial R_{pred}}{\partial R^i_A} \equiv \begin{cases} 1, & \text{if } C_A \neq 0 \\ 0, & \text{if } C_A = 0 \end{cases}$$

$$\begin{aligned} \dot{x}_1 &= C_A(R_{max} - R_{AB}) - (k_a C_A + k_d)x_1 \\ \dot{x}_2 &= -R_{AB} - (k_a C_A + k_d)x_2 \\ \dot{x}_3 &= k_a C_A - (k_a C_A + k_d)x_3 \end{aligned}$$

Optimization of experiments

The main objective of this manuscript is, given a quantity of analyte, to find the shortest experiment that will provide a desired standard error in the estimated values of the interaction rate constants k_a and k_d. Optimum design of experiments have been studied in the past using various techniques. Many optimality criteria have been used to define the optimization problem in the literature: the A-optimality (Montgomery, 2005), the E-optimality (Lorenzen and Anderson, 1993), and the D-optimality (Pronzato and Walter, 1989). Let the p eigenvalues of the inverse of the Hessian be denoted by λ_i. The A-optimality criterion minimizes the average variance, that is, it maximizes the trace of the inverse of the Hessian, that is, max ($\Sigma\lambda_i$). The E-optimality criterion minimizes the maximum variance of the parameters, that is, maximizes the minimum eigenvalue of the inverse of the Hessian, that is, max (min λ_i). The D-optimality criterion minimizes the volume of the space in which the

Journal of Molecular Recognition

estimated parameters could lie. This corresponds to maximizing the determinant of the inverse of the Hessian, that is, max ($\Pi\lambda_i$).

In this paper, the novelty lies in the formulation of the optimization problem, which is motivated by the user requirements rather than a variance criterion as discussed before. The problem is to minimize the experimentation time subject to the desired standard errors acting as constraints. In addition, physical limitations such as finite analyte quantity are also taken into consideration. The optimization problem is then defined as follows:

$$\begin{aligned} &\min_{t_{on},t_{off},C_A} (t_{on} + t_{off}) \\ &s.t. \quad \xi_a \le \beta_a,\ \xi_b \le \beta_b,\ t_{on} + t_{off} \le T_{max} \\ &\qquad C_A t_{on} \le \eta_{max},\ C_A \le C_{max} \end{aligned} \tag{3}$$

where t_{on} and t_{off} are the association and the dissociation periods of the experiment, respectively, C_A the concentration of analyte to inject, β_a and β_d are the desired standard errors in estimated parameters k_a and k_d, respectively, η_{max} and C_{max} are the maximum amount and concentration of analyte allowed to be used, and T_{max} the maximum total time allowed for the experiment. The standard errors ξ_a and ξ_d are computed based on the Hessian information.

As with any experimental design, the values of k_a and k_d need to be known to choose the optimum experiment. This, however, is not possible (if the true values were known, there would be no reason to perform an experiment!) and so, the optimum design is based on a previous non-optimized experiment. So, the algorithm utilized can be written as follows:

1. Perform a first non-optimized experiment with arbitrarily chosen t_{on}, t_{off}, and C_A.
2. Compute the parameter values k_a, k_d and the associated standard errors.
3. Optimize the second experiment by numerically solving the optimization problem presented in Equation (3).
4. If the optimization does not lead to a feasible solution, increase the number of experiments in the optimization formulation. Increase until a feasible solution is obtained.
5. Once a feasible solution is found, perform the second set of optimized experiments.
6. Compute the parameter values and the associated standard errors taking the data from the two sets of experiments (i.e., non-optimized and optimized injections) into account.
7. If the final obtained standard errors are not satisfactory repeat steps 3–6.

MATERIALS AND METHODS

Materials

Phosphate buffer saline (PBS, 10 mM, pH 7.4) was from Invitrogen (USA). Biacore 3000™ and Biacore T100™ optical biosensors, HBS-EP buffer, research grade CM5 and CM4 sensorchips, 10 mM glycine solution (pH 2.0), Tween-20 surfactant, amine and thiol coupling kit solutions were from BIACORE Inc. (Piscataway, NJ, USA). Soluble, recombinantly expressed and purified prostate-specific membrane antigen (PSMA, 50 000 Da), purified anti-PSMA mouse monoclonal IgG antibody (clone #17G1, 1 mg ml^{-1} in PBS/10% glycerol), denoted below as mAb, were gifts from Dr S. Moffett (Proscan RX Pharma Inc., Montreal, Quebec, Canada). PS0215 (CGKSLYESWTKK) and Kcoil peptides (sequence: CGG(KVSALKE)$_5$) were chemically synthesized by Bio-Synthesis Inc., Lewisville, TX, USA (95% purity). Ecoil-EGF, a chimeric protein corresponding to the epidermal growth factor (EGF) being N-terminally tagged with a His-tag and with the Ecoil peptide (sequence (EVSALEK)$_5$) were produced in-house by transient transfection of HEK-293 cells and purified by standard IMAC chromatography. Purity was estimated to be higher than 90% by SDS–PAGE followed by Coomassie staining (data not shown).

Biosensor surface preparation

Biacore 3000 protocols

PSMA was covalently immobilized to the surface of a CM5 sensorchip using standard amine coupling procedure with HBS-EP as running buffer. Briefly, activation of the sensorchip surface was performed by injecting an equimolar solution of *N*-ethyl-*N*′-(3-dimethyl aminopropyl)-carbodiimide hydrochloride and *N*-hydroxysuccinimide at a flow rate of 5 μl min^{-1} for 10 min. PSMA, diluted in 10 mM acetate buffer, pH 5.0 was manually injected until 400 RU of protein was coupled. The remaining activated groups were then deactivated by injecting ethanolamine-HCl solution for 10 min. In addition to PSMA-derivatized surface, a mock surface was generated using the same protocol in which PSMA injection was replaced by buffer injection. After PSMA and mock surface preparation, the sensorchip surfaces and integrated fluidic cartridge of the instrument were rinsed extensively with filtered degased PBS/0.005% Tween-20 solution that has been subsequently used as running buffer for kinetic experiments as well as for mAb dilution.

Biacore T100 protocols

PS0215 and Kcoil peptides were covalently immobilized to the surfaces of CM4 sensorchips using standard thiol coupling procedure with HBS-EP as running buffer, as previously described (De Crescenzo *et al*., 2003). For each peptide, less than 10 RU were covalently coupled to each surface. Mock surfaces were also generated using the same protocol (no peptide injection). HBS-EP buffer was then used as a running buffer for all subsequent experiments as well as for analyte dilution.

Kinetic profile generation and analysis

Biosensor-based kinetic measurements were performed at 25°C with a data acquisition rate of 10 Hz.

PSMA/mAb interactions

The experimental "reference" profile was obtained as follows: independent 1:2 dilutions of mAb (ranging from 18.75 to 300 nM) as well as running buffer were then injected for 240 s at a flow rate of 30 μl min^{-1} (two independent duplicates). Each injection was followed by a buffer injection for 360 s in order to record the dissociation of PSMA-mAb complexes. In between injections, sensorchip surfaces were regenerated with three pulses of glycine solution (20 s each at 100 μl min^{-1}) followed by an EXTRACLEAN procedure in order to elute surface-bound antibody and clean the instrument for subsequent injections, respectively. Sensorgrams were then control-corrected using a double-referencing procedure (Rich and Myszka, 2000) prior to global analysis in BIAevaluation 3.1 software package provided with the Biacore 3000™ instrument using a simple binding model. Signal corresponding to the first 5 s on mAb injection and to 3 s prior

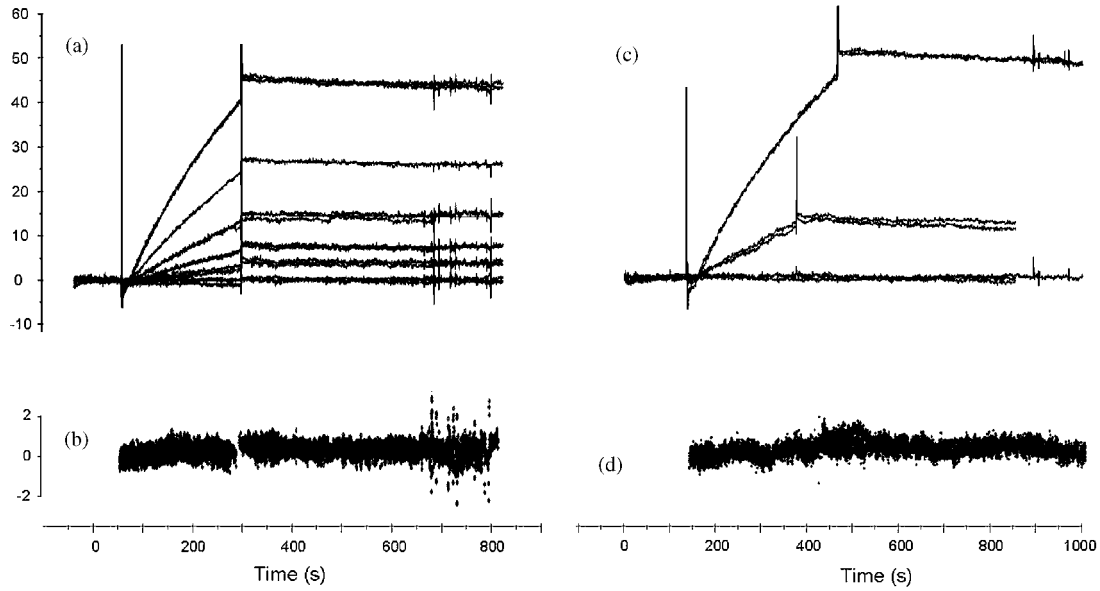

Figure 1. mAb/PSMA interactions. Double-referenced experimental data sets and related residuals corresponding to non-optimized injections (a, b) and to online optimized injections (c, d) of anti-PSMA monoclonal antibody over a PSMA-immobilized surface. Injections were performed in duplicate. Parameters for the different injections are given in the text.

and after buffer injection performed for monitoring complex dissociation were not taken into account for global analysis.

PS0215/mAb interactions

After three cycles of buffer injection and generation for conditioning the surface, the reference profile was obtained as follows: independent 1:2 dilutions of mAb (ranging from 12.5 to 100 nM, single injections) as well as running buffer (duplicate) were then injected for 180 s at a flow rate of 30 μl min^{-1}. Each injection was followed by a buffer injection for 360 s. In between injections, sensorchip surfaces were regenerated with three pulses of glycine solution (20 s each at 100 μl min^{-1}). Sensorgrams were automatically control-corrected and double-referenced using the Biacore T100 evaluation software (version 1.1.1) prior to global analysis using a simple binding model.

Kcoil/Ecoil-EGF interactions

After three cycles of buffer injection and generation for conditioning the surface, the reference profile was obtained as follows: independent 1:2 dilutions of Ecoil-EGF (ranging from 18.75 to 300 nM, independent duplicate) as well as running buffer (triplicate) were then injected for 60 s at a flow rate of 100 μl min^{-1}. Each injection was followed by a buffer injection for 120 s. In between injections, sensorchip surfaces were regenerated with one pulse of 5 M guanidium HCl (20 s at 100 μl min^{-1}). Sensorgrams were automatically control-corrected and double-referenced using the Biacore T100 evaluation software (version 1.1.1) prior to global analysis using a simple binding model.

Simulations and optimization

Simulations, profile optimization, and analyses of simulated data were performed using an in-house program developed with MATLAB 7.0 software platform (The Mathworks, Natick, MA, USA) using a simple Langmuirian kinetic model. Parameters used for the generation of simulated "reference" profiles corresponded to 240 s of protein injection and 360 s of complex dissociation. For reference profile, the concentration series used in all simulations was 300, 150, 75, 37.5, and 18.75 nM (1:2 dilutions of mAb ranging from 18.75 to 300 nM). Twenty scenarios were considered, which represented the combinations of k_a (10^4, $10^{4.5}$, 10^5, $10^{5.5}$, and 10^6 M^{-1} s^{-1}) and k_d (10^{-5}, 10^{-4}, 10^{-3}, 10^{-2} s^{-1}). Given a combination of the parameter values, the profiles were generated by solving the differential equations. The value of R_{max} was then adjusted for each scenario such that, at the end of an injection of 300 nM, the resonance value was 50 RU. Secondly, the noise part was derived from experimental data shown in Figure 1a as follows. The difference between experimental and calculated data was considered as the noise. This noise was added to the simulated data so as to resemble real biosensor data. This noise was close to being Gaussian, though certain non-Gaussian behavior was sighted at certain specific time, thereby motivating the above strategy of noise addition.

For the optimization, the standard sequential quadratic programming algorithm that is integrated with MATLAB was used. One of the key elements was the calculation of the standard deviation of the measurement noise, σ. Note that the error between the model and the real data is the result of two different sources: the machine noise (including artifacts such as refractive index mismatches) and the noise related to sample preparation. In this paper, only the error in the parameters caused by the machine is addressed. The variation in the parameters due to sample preparation is supposed to be compensated by performing the experiments in duplicate, a regular practice for biological systems. To isolate the machine noise, each experiment was identified individually and then the difference between the measured and the predicted values was used as an indicative of the machine noise. Then, an average of this indicative over the five different experiments was obtained. Here, a noise standard deviation of 0.3 RU was computed. This value has been used for all calculations of the standard errors.

Journal of Molecular Recognition

RESULTS

Preliminary experimental data and optimization

We hypothesized that a numerical online optimization strategy would be as efficient as a traditional experimental plan in terms of kinetic parameter determination (values and related confidence levels) for the characterization of macromolecular interactions by an SPR-based biosensor approach, while minimizing experimental time and material consumption. This hypothesis was first tested experimentally by recording a set of sensorgrams corresponding to the interactions of a monoclonal antibody (the analyte) with its antigen (PSMA, the ligand) that had been previously immobilized on our biosensor surface. The data corresponding to a non-optimized experimental approach (i.e., range of concentration selected *a priori*; duplicate injections corresponding to 1:2 dilutions; fixed duration time for each injection and dissociation phase) were then control-corrected, doubled-referenced (Figure 1a), and globally analyzed using a simple Langmuirian model available in Biaevaluation 3.1 and our in-house software packages. As can be seen in Figure 1a, double-referenced data still presented refractive index mismatches at some injection starts. As already discussed by Cannon *et al.* (2004), these mismatches more likely result from the fact that flowcells within the Biacore 3000™ instrument are connected in series. This causes a dispersion of the sample plug during injection. The resulting spikes, however, did not impact subsequent data analysis since these data points were eliminated prior to globally fitting the data and since a local correction factor (R_A^i) was also introduced to take this artifact into account. The experimental data (Figure 1a) were globally analyzed and were found to be well depicted by a simple kinetic model with residuals almost randomly distributed over a zero value (Figure 1b). Table 1 shows the set of kinetic parameters and their associated confidence levels as determined with both software packages.

Our online optimization strategy was then evaluated as follows. In the first step, the injections corresponding to buffer and to the mid-range concentration of analyte (i.e., 75 nM) were repeated in duplicate using the same experimental conditions as in the reference experiment. These sensorgrams were then prepared as described above and were used to predict the optimal injection to be performed in order to satisfy the following criterion: the levels of confidence for each kinetic parameter should be lower than or equal to those determined for the reference profile while satisfying both constraints: (i) the total amount of injected protein for the optimized experiment should be lower than or equal to that used in the reference profile and the maximal concentration of protein to be injected should be lower than or equal to the maximal concentration used, that is, 300 nM; (ii) the total duration of the experiment should be lower than or equal to that of the reference profile.

The computed optimal profile was to inject the analyte at its maximum concentration for a period of 330 s and to let the dissociation occur for 530 s (buffer injection whose duration matched that of the optimized injection for double referencing purpose were taken into account in the optimization calculation). The optimized experiment was then performed (Figure 1c) and the related set of sensorgrams (including the first non-optimized sensorgrams) was analyzed as performed previously for the non-optimized reference profile (Figure 1d). As can be seen in Table 1, in that specific case, our optimization approach was successful as one can judge by comparing the values of kinetic parameters as well as the related standard errors obtained when globally analyzing the optimized and reference data sets. Furthermore, our optimized strategy allowed for a reduction of both protein amount (234 vs. 279 pmol) and experimentation time (178 min for the online optimized data set versus 316 min for the non-optimized data set). Due to the bivalent nature of our mAb, the excellent adequation between experimental data and a simple kinetic model was surprising. Indeed, one would have expected that multiple interactions between one mAb and two antigens might occur simultaneously. Similar cases of good adequation between global fits with a simple model and experimental data that were expected to deviate from such a simple model have already been reported (Svitel *et al.*, 2003; Rich *et al.*, 2008). In our case, it is more likely that additional binding events leading to the formation of a 2:1 stoichiometry complex may occur on a different time-scale than the one explored in both non-optimized and optimized experiments.

Further experimental validation of the optimization strategy using a Biacore T100 instrument

Two additional biological systems were then used to validate our numerical optimization strategy as well as to test its performance with low levels of noise provided by the new generation of SPR biosensors from BIACORE Inc. The selected biological systems corresponded to (a) the interactions of our monoclonal antibody with PS0215, that is, its 12 amino acid-long linear epitope (Moffett *et al.*, 2007) and (b) the interactions between Ecoil-EGF, a chimeric protein corresponding to the epidermal growth factor (EGF)

Table 1. Kinetic parameters determined for non-optimized (reference) and online optimized profile using BIAevalution 3.1 and in-house software for the interactions of mAb with PSMA

	Reference profile		Optimized profile	
Software	BIAeval 3.1	In-house	BIAeval 3.1	In-house
k_a ($10^4\,M^{-1}\,s^{-1}$) $\pm\,\xi$	1.07 ± 0.0015	1.07 ± 0.0014	0.87 ± 0.0019	0.88 ± 0.0015
k_d ($10^{-4}\,s^{-1}$) $\pm\,\xi$	0.648 ± 0.008	0.650 ± 0.009	0.97 ± 0.009	1.2 ± 0.007
R_{max} (RU) $\pm\,\xi$	84.4 ± 0.1	87 ± 0.1	93.2 ± 0.15	91 ± 0.1
η_a (pmol)	279	279	234	234
T (min)	316	316	178	178

η_a, total analyte consumption; T, total experimental time.

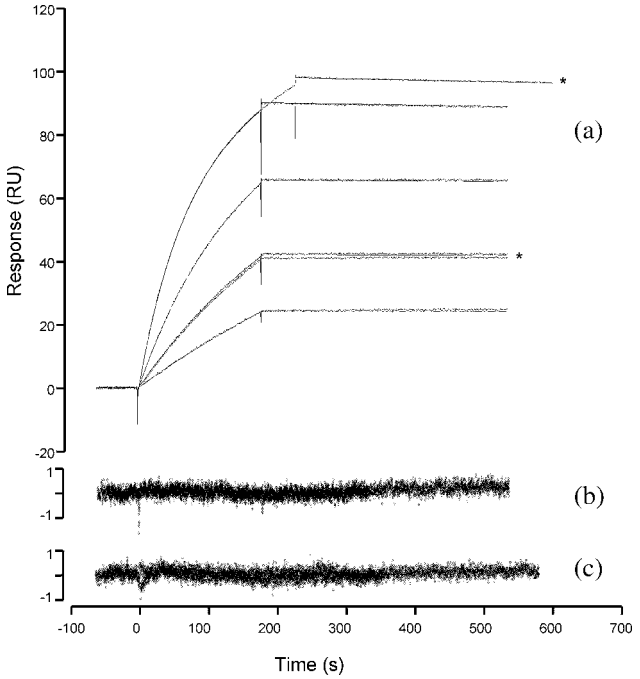

Figure 2. mAb/PS0215 interactions. Double-referenced experimental data sets (a) corresponding to non-optimized (12.5, 25, 50, 100 nM) and optimized set of injections (25, 100 nM, labeled with *) of anti-PSMA monoclonal antibody over a PS0215-immobilized surface. Related residuals are shown in (b) and (c), respectively. Parameters for the different injections are given in the text. Single injections for the non-optimized and optimized data sets were performed, note, however, the high quality of the data as 12.5 and 100 nM injections that are common to both data sets are almost superimposable.

being N-terminally tagged with a *de novo* designed peptide (the Ecoil) known to specifically interact with its coil partner (Kcoil) and form a heterodimeric coiled-coil complex (De Crescenzo *et al.*, 2003).

Table 2. Kinetic parameters determined for non-optimized (reference) and online optimized profile using the Biacore T100 Evaluation software (version 1.1.1) for the interactions of mAb with PS0215

	Reference profile	Optimized profile
k_a ($10^5\,M^{-1}\,s^{-1}$) $\pm\,\xi$	1.2 ± 0.1	1.11 ± 0.01
k_d ($10^{-5}\,s^{-1}$) $\pm\,\xi$	1.9 ± 0.2	2.5 ± 0.2
R_{max} (RU) $\pm\,\xi$	101.20 ± 0.07	106.10 ± 0.06
η_a (pmol)	16.8	13.7
T (min)	76	53

η_a, total analyte consumption; T, total experimental time.

Experiments were conducted with a Biacore T100™ instrument known to provide better reproducibility and sensitivity when compared to the Biacore 3000™ model. In both cases, low amounts of peptides, that is, less than 10 RUs of PS0215 or Kcoil peptides, both displaying an engineered cysteine at their N-termini were immobilized onto different biosensor surfaces using thiol coupling protocol. In both cases, protocols related to non-optimized injections of each analyte were generated using the software wizard of the biosensor instrument and further analyzed with the Biacore T100 evaluation software. In both cases, these non-optimized data sets (Figures 2a and 3a) were well depicted by a 1:1 binding model (see residuals in Figures 2b and 3b). Kinetic parameters related to these interactions are given in Tables 2 and 3, respectively.

Our online optimization strategy was then applied by providing our software with the sensorgrams corresponding to the injections performed at 25 or 18.75 nM with mAb and Ecoil-EGF analytes, respectively. The software was required to predict the optimal profile obeying the same criterion and satisfying the same constraints as before. The optimal injections were determined to be of 100 nM for mAb with [analyte; buffer] durations of [230 s; 375 s] (instead of [180 s; 360 s] for the

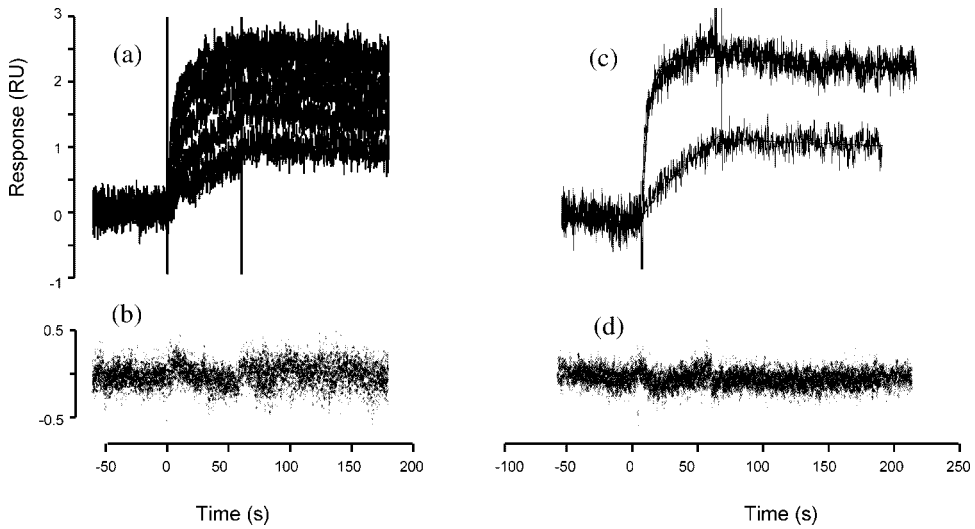

Figure 3. Ecoil-EGF/Kcoil interactions. Double-referenced experimental data sets and related residuals corresponding to non-optimized injections (a, b) and to online optimized injections (c, d) of Ecoil-EGF over a Kcoil peptide-immobilized surface. Injections were performed in duplicate. Parameters for the different injections are given in the text.

Journal of Molecular Recognition

Table 3. Kinetic parameters determined for non-optimized (reference) and online optimized profile using the Biacore T100 Evaluation software (version 1.1.1) for the interactions of Ecoil-EGF with Kcoil peptide

	Reference profile	Optimized profile
k_a ($10^5\,M^{-1}\,s^{-1}$) $\pm\xi$	5.2 ± 0.1	7.03 ± 0.09
k_d ($10^{-4}\,s^{-1}$) $\pm\xi$	6.2 ± 0.4	7.3 ± 0.6
R_{max} (RU) $\pm\xi$	2.7 ± 0.1	2.64 ± 0.02
η_a (pmol)	116	64
T (min)	86	34

η_a, total analyte consumption; T, total experimental time.

non-optimized injections) and of 300 nM for Ecoil-EGF with [analyte; buffer] durations of [55 s; 150 s] (instead of [60 s; 120 s] for the non-optimized injections).

The optimized profiles were then tested by repeating the non-optimized 25 nM mAb and 18.75 nM Ecoil-EGF injections in addition to the optimized injections proposed by the software. Buffer injections at matching time for double referencing purpose were also performed. The experimental optimized sets of sensorgrams are shown in Figure 2a (sensorgrams labeled with *) for mAb and Figure 3c for Ecoil-EGF. These optimized profiles were then globally analyzed with the Biacore T100 evaluation software using a 1:1 binding model. The latter adequately described the experimental data (see related residuals in Figures 2c and 3d). Kinetic parameters related to the optimized profiles (Tables 2 and 3) were found to be in excellent agreement with those derived from the global analysis of the non-optimized data sets. As previously observed with Biacore 3000 data sets, our optimization approach was thus successful since it allowed for a significant reduction of both protein amount and experimentation time in both cases (Tables 2 and 3).

Simulated data and optimization

In order to further evaluate the applicability and the potential gains resulting from the implementation of our strategy, a simulation approach was undertaken as we do not have in our laboratory all the macromolecular systems that would cover a huge range of kinetic parameter values. Hence, data sets corresponding to the different combinations of association rates (k_a) varying from 10^4 to $10^6\,M^{-1}\,s^{-1}$ and dissociation rates (k_d)

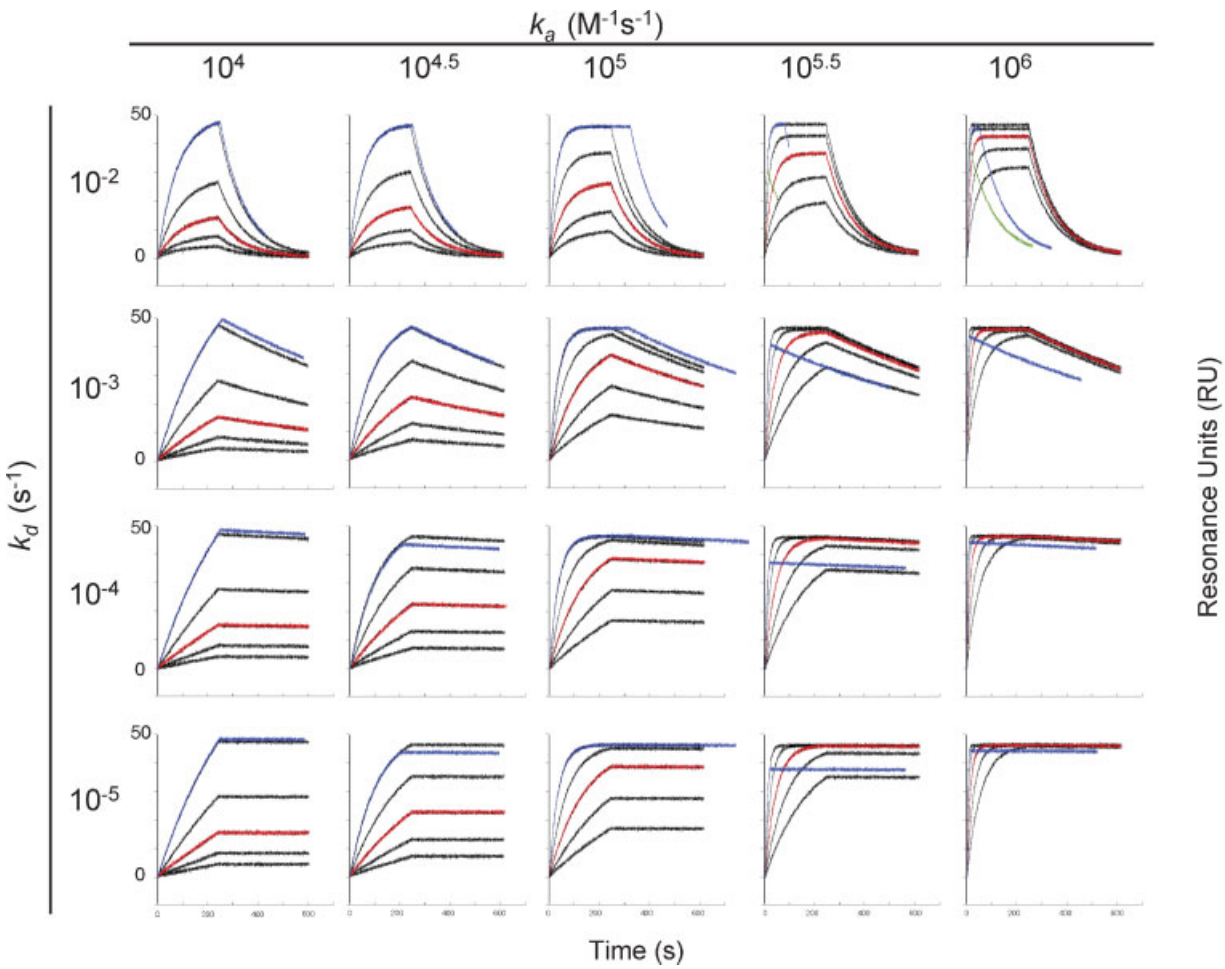

Figure 4. Simulated data sets corresponding to various combinations of k_a and k_d constants. Non-optimized sensorgrams corresponding to arbitrarily chosen injections are shown in black and red while sensorgrams corresponding to online optimized injections are shown in blue and green.

varying from 10^{-2} to $10^{-5}\,s^{-1}$ were generated. For each combination of kinetic parameters, sensorgrams corresponding to five injections of analyte (same concentrations as in our experimental reference profile shown in Figure 1) were simulated using a simple model of interactions. Each simulated data set was then normalized so that the maximal accumulation of analyte corresponded to 50 RU (approximately the same amount as in our experimental reference profile). Experimental noise corresponding to the residuals shown in Figure 1b was then added to better mimic experimental data. Figure 4 shows the different sets of sensorgrams hence generated (shown in black and red in all the panels). After noise addition, each data set was globally analyzed, as normally performed with real data (i.e., k_a, k_d, and R_{max} being considered as global parameters to be determined), in order to determine the levels of confidence associated to each kinetic parameter. Initial values of $10^5\,M^{-1}\,s^{-1}$, $10^{-3}\,s^{-1}$ and 100 RUs for k_a, k_d, and R_{max}, respectively, were provided to the software in order to start the iterative process for global fitting (these values corresponded to those used as default in the Biaevaluation software).

It is important to note that the various parameters are indeed correlated. For example, correlation could be expected between k_a and R_{max} when the data are almost linear. Thus, the curvature in data is essential to be able to estimate the parameters with a reasonable standard error. For every data set shown in Figure 4, the software gave parameter values close to those used to generate the data. The standard errors for k_a and k_d are given in Table 4. The saturation level was also obtained quite precisely with less than 0.1% standard error, except in the case of the data set corresponding to (k_a; k_d) equal to ($10^4\,M^{-1}\,s^{-1}$; $10^{-2}\,s^{-1}$) for which the standard error was 0.3%. Hence, despite the little curvature in the injection phase of some simulated data sets, their global analysis provided good-enough accuracy on all the estimated parameters. This shows that the correlation between the various parameters did not bias the analysis.

Our online optimization strategy was then tested, in a manner identical to that performed with the experimental data set, that is, by providing our in-house software with one non-optimized sensorgram (corresponding to analyte concentration of 75 nM; shown as red sensorgrams in all panels of Figure 4) and the same optimization criterion, that is, confidence levels equal to those obtained with the non-optimized data set (listed in Table 4) and the same constraints as previously. In all the cases, the software was able to find a solution to the problem by proposing experimental parameters for a single optimized injection (shown as blue sensorgram in all panels of Figure 4) or, in two cases, by proposing two distinct injections at different concentrations (in those cases, the sensorgram corresponding to the second injection is shown in green in Figure 4 panels). As in the case of non-optimized experiments, a global analysis of the optimized profiles (noise added) gave values of k_a, k_d, and R_{max} in excellent agreement with those used to generate the data.

A close examination of Figure 4 highlights that the optimized injections proposed by the software were, as expected, highly dependent on the kinetic values of the simulated macromolecular interactions. That is, when the interactions were characterized by k_a values in between 10^4 and $10^5\,M^{-1}$ combined with k_d values between 10^{-2} and $10^{-5}\,s^{-1}$, the optimized profile implied the use of the highest concentration allowed (300 nM) in order to reach, or at least approach equilibrium (and, if possible, saturation) during the injection. In these cases, confidence levels on both kinetic parameters was less than 0.1%, except for k_d values equal to $10^{-5}\,s^{-1}$ for which confidence levels higher than 8% were determined (Table 4). These results are in perfect agreement with previous conclusions from Önell and Andersson (2005) who experimentally demonstrated that reliable kinetics determination requires at least two sensorgrams associated with different sample concentrations and displaying sufficient curvature with at least one reaching equilibrium with more than 90% saturation during sample injection.

Table 4. Evaluation of the performance of the online optimization strategy

	k_a ($M^{-1}\,s^{-1}$)				
k_d (s^{-1})	10^4	$10^{4.5}$	10^5	$10^{5.5}$	10^6
10^{-2}	ξ_a: 0.0033×10^4 ξ_d: 0.00045×10^{-2} TR: 2.3	ξ_a: $0.0013 \times 10^{4.5}$ ξ_d: 0.00043×10^{-2} TR: 2.3	ξ_a: 0.0008×10^5 ξ_d: 0.00038×10^{-2} TR: 2.3	ξ_a: $0.0007 \times 10^{5.5}$ ξ_d: 0.00033×10^{-2} TR: 3.2	ξ_a: 0.0008×10^6 ξ_d: 0.00030×10^{-2} TR: 2.0
10^{-3}	ξ_a: 0.0012×10^4 ξ_d: 0.00097×10^{-3} TR: 2.0	ξ_a: $0.0005 \times 10^{4.5}$ ξ_d: 0.00086×10^{-3} TR: 2.0	ξ_a: 0.0003×10^5 ξ_d: 0.00070×10^{-3} TR: 1.8	ξ_a: $0.0003 \times 10^{5.5}$ ξ_d: 0.00060×10^{-3} TR: 2.2	ξ_a: 0.0006×10^6 ξ_d: 0.00057×10^{-3} TR: 2.3
10^{-4}	ξ_a: 0.0010×10^4 ξ_d: 0.0082×10^{-4} TR: 2.0	ξ_a: $0.0004 \times 10^{4.5}$ ξ_d: 0.0073×10^{-4} TR: 2.0	ξ_a: 0.0002×10^5 ξ_d: 0.0058×10^{-4} TR: 1.8	ξ_a: $0.0003 \times 10^{5.5}$ ξ_d: 0.0049×10^{-4} TR: 2.1	ξ_a: 0.0006×10^6 ξ_d: 0.0047×10^{-4} TR: 2.2
10^{-5}	ξ_a: 0.0010×10^4 ξ_d: 0.0815×10^{-5} TR: 2.0	ξ_a: $0.0004 \times 10^{4.5}$ ξ_d: 0.0724×10^{-5} TR: 2.0	ξ_a: 0.0002×10^5 ξ_d: 0.0572×10^{-5} TR: 1.8	ξ_a: $0.0003 \times 10^{5.5}$ ξ_d: 0.0485×10^{-5} TR: 2.1	ξ_a: 0.0006×10^6 ξ_d: 0.0467×10^{-5} TR: 2.2

ξ_a, standard error on k_a; ξ_d, standard error on k_d. ξ_i were determined by globally analyzing simulated data sets and were used as targeted values when applying our online optimization strategy. TR, time ratio defined as the duration of the non-optimized data set (corresponding to black and red sensorgrams in Figure 4) in addition to a buffer injection for double referencing purpose, divided by duration of the online optimized injections (corresponding to the red, blue, and green sensorgrams in Figure 4) in addition to buffer injections matching the duration of the optimized profiles for double referencing purpose.

Following the same reasoning, for sets of sensorgrams corresponding to k_a values higher than $10^{5.5}\,M^{-1}\,s^{-1}$ and k_d values lower than $10^{-3}\,s^{-1}$, 90% of surface saturation was reached with the non-optimized initial injection itself (Figure 4). The solution proposed by the software was to limit both concentration and injection duration in order to maximize the duration of the sensorgram portion corresponding to dissociation (and thus rapidly satisfy the constraint on k_d confidence level).

Of interest, for fast association/dissociation systems, that is, k_a values higher than $10^{5.5}\,M^{-1}\,s^{-1}$ combined to k_d values equal to $10^{-2}\,s^{-1}$, two optimized injections were required in order to obtain confidence levels as good as those determined for the non-optimized profile (Figure 4). This requirement is more likely imposed by the high value of k_a that limited the number of points during the transient phase associated to mass accumulation as well as by the k_d/k_a ratio (i.e., the thermodynamic dissociation constant, K_d) being too low to allow for 90% saturation during the first non-optimized injection. Also, in the case of interactions characterized by fast on-rates (i.e., higher than $10^{5.5}\,M^{-1}\,s^{-1}$, last column in Figure 4), mass transport limitation phenomenon (i.e., limiting diffusion of the analyte from the bulk to the vicinity of the surface) has been previously reported to noticeably affect sensorgram profile (Myszka *et al*., 1998). This artifact was not modeled in our simulation. It is however expected that the use of a more complex kinetic model to take that phenomenon into account may negatively affect both confidence levels and parameter correlations. This issue has to be addressed to extend our strategy to biological interactions with fast on-rate.

DISCUSSION

It is now well accepted that surface plasmon resonance-based BIACORE instruments allow for reliable kinetic characterization of almost all biological interactions involving macromolecules. A reliable characterization, however, requires a careful optimization of key parameters such as selecting the appropriate coupling chemistry, limiting the amount of ligand to be captured or immobilized, optimizing protocols to ensure complete surface regeneration without, however, affecting ligand integrity, etc., as well as rigorous controls such as buffer injections and double referencing protocols prior to data analysis. Those aspects have already been extensively discussed and guidance in those endeavors is available (O'Shannessy and Winzor, 1996; Karlsson and Fält, 1997; Andersson *et al*., 1999; Rich and Myszka, 2000). In this study, we obeyed these rules; that is, sets of experimental sensorgrams generated with our Biacore instruments and simulated data (to which experimental noise had been added) presented a good compromise between unfavorable signal-to-noise ratio (Ober and Ward, 1999) and favorable conditions for limiting mass transport artifacts and surface heterogeneities (Karlsson and Larsson, 2004).

Another important parameter that may limit the accuracy of kinetic constants determination is the availability of ligand samples being highly pure, aggregate-free, and highly concentrated. This last requirement is often violated when samples are costly or when they are in-house produced at low scale. We thus limited ourselves to analyte injections (and simulations) corresponding to total analyte consumption being less than 300 pmol and concentrations being in the 100 nM range. We then demonstrated that the information-rich nature of real-time data from SPR biosensors can be exploited, in combination with a careful, fully automated experimental design, to get comparable accuracy and confidence on kinetic parameters as those derived from non-optimized (i.e., time and material consuming) experimental data sets traditionally collected. Indeed our results indicated that, when the interactions follow a simple mode of binding, one or two carefully planned injections are enough to reach confidence levels similar to those derived from non-optimized experimental data. This is in perfect agreement with previous results from Önell and Andersson (2005). The novelty of our approach, however, relies on the development of an algorithm that was shown to efficiently predict, using one single non-optimized sensorgram, the experiments to be performed in order to determine kinetic parameters with the desired levels of confidence. Overall, the application of our online optimization algorithm led to a significant reduction of experiment time as evaluated by the time ratio parameter, TR, varying from 1.8 to 3.2 (Table 4).

In combination with advanced experimental protocols (such as ligand capture approaches) and data treatment algorithms allowing for automated double-referencing, our strategy can be easily implemented to perform injections in an automated fashion and thus significantly reduce machine time and sample consumption to accommodate high-throughput kinetic characterization. Furthermore, our strategy can be easily adapted to more complex binding mechanisms, for example, by taking into account mass transport limitations.

Acknowledgements

GDC is a Canada Research Chairholder (CRC on Protein-enhanced Biomaterials, tier 2 level). This research was supported by NSERC grants to GDC and BS.

REFERENCES

Andersson K, Hamalainen M, Malmqvist M. 1999. Identification and optimization of regeneration conditions for affinity-based biosensor assays. A. multivariate cocktail approach. *Anal. Chem.* **71**: 2475–2481.

Ben Khalifa M, Choulier L, Lortat-Jacob H, Altschuh D, Vernet T. 2001. BIACORE data processing: an evaluation of the global fitting procedure. *Anal. Biochem.* **293**: 194–203.

Cannon MJ, Papalia GA, Navratilova I, Fisher RJ, Roberts LR, Worthy KM, Stephen AG, Marchesini GR, Collins EJ, Casper D, Qiu H, Satpaev D, Liparoto SF, Rice DA, Gorshkova II, Darling RJ, Bennett DB, Sekar M, Hommema E, Liang AM, Day ES, Inman J, Karlicek SM, Ullrich SJ, Hodges D, Chu T, Sullivan E, Simpson J, Rafique A, Luginbuhl B, Nyholm Westin S, Bynum M, Cachia P, Li YJ, Kao D, Neurauter A, Wong M, Swanson M, Myszka DG. 2004. Comparative analyses of a small molecule/enzyme interaction by multiple users of Biacore technology. *Anal. Biochem.* **330**: 98–113.

Day YSN, Baird CL, Rich RL, Myszka DG. 2002. Direct comparison of binding equilibrium, thermodynamic and rate constants determined by surface- and solution-based biophysical methods. *Prot. Sci.* **11**: 1017–1025.

De Crescenzo G, Grothe S, Lortie R, Debanne MT, O'Connor-McCourt MD. 2000. Real-time kinetic studies on the interaction of transforming growth factor alpha with the epidermal growth factor receptor extracellular domain reveal a conformational change model. *Biochemistry* **39**: 9466–9476.

De Crescenzo G, Litowski JR, Hodges RS, O'Connor-McCourt MD. 2003. Real-time monitoring of the interactions of two-stranded de novo designed coiled-coils: effect of chain length on the kinetic and thermodynamic constants of binding. *Biochemistry* **42**: 1754–1763.

De Crescenzo G, Pham PL, Durocher Y, Chao H, O'Connor-McCourt MD. 2004. Enhancement of the antagonistic potency of TGF-beta receptor extracellular domains by coiled-coil induced homo- and heterodimerization. *J. Biol. Chem.* **279**: 26013–26018.

De Crescenzo G, Hinck CS, Shu Z, Zuniga J, Yang J, Tang Y, Baardsnes J, Mendoza V, Sun L, Lopez-Casillas F, O'Connor-McCourt MD, Hinck AP. 2006. Three key residues underlie the differential affinity of the TGFβ isoforms for the type II receptor. *J. Mol. Biol.* **355**: 47–62.

DiGiacomo RA, Xie L, Cullen C, Indelicato SR. 2004. Development and validation of a kinetic assay for analysis of anti-human interleukin-5 monoclonal antibody (SCH 55700) and human interleukin-5 interactions using surface plasmon resonance. *Anal. Biochem.* **327**: 165–175.

Fägerstam LG, Frostell A, Karlsson R, Kullman M, Larsson A, Malmqvist M, Butt H. 1990. Detection of antigen–antibody interactions by surface plasmon resonance: applications to epitope mapping. *J. Mol. Recognit.* **3**: 208–214.

Fisher RJ, Fivash M, Casas-Finet J, Erickson JW, Kondoh A, Bladen SV, Fisher C, Watson D, Papas T. 1994. Real-time DNA binding measurements of the ETS1 recombinant oncoproteins reveal significant kinetic differences between the p42 and p51 isoforms. *Prot. Sci.* **3**: 257–266.

Karlsson R, Fält A. 1997. Experimental design for kinetic analysis of protein–protein interactions with surface plasmon resonance biosensors. Affinity measurements using surface plasmon resonance. *J. Immunol. Meth.* **200**: 121–133.

Karlsson R, Larsson A. 2004. Affinity measurements using surface plasmon resonance. *Meth. Mol. Biol.* **248**: 389–415.

Kikuchi Y, Uno S, Nanami M, Yoshimura Y, Iida S, Fukushima N, Tsuchiya M. 2005. Determination of concentration and binding affinity of antibody fragments by use of surface plasmon resonance. *J. Biosci. Bioeng.* **100**: 311–317.

Kozlov G, De Crescenzo G, Lim NS, Siddiqui N, Fantus D, Kahvejian A, Trempe J-F, Elias D, Ekiel I, Sonenberg N, O'Connor-McCourt MD, Gehring K. 2004. Structural basis of ligand recognition by PABC, a highly specific peptide-binding domain found in poly(A)-binding protein and a HECT ubiquitin ligase. *EMBO J.* **23**: 272–281.

Krogsgaard M, Prado N, Adams EJ, He XL, Chow DC, Wilson DB, Garcia KC, Davis MM. 2003. Evidence that structural rearrangement and/or flexibility during TCR binding can contribute to T cell activation. *Mol. Cell.* **12**: 1367–1378.

Lenferink AE, van Zoelen EJ, van Vugt MJ, Grothe S, van Rotterdam W, van de Poll ML, O'Connor-McCourt MD. 2000. Superagonistic activation of ErbB1 by EGF-realted growth factors with enhanced association and dissociation rate constants. *J. Biol. Chem.* **275**: 36748–36753.

Lim NS, Kozlov G, Chang TC, Groover O, Siddiqui N, Volpon L, De Crescenzo G, Shyu A-B, Gehring K. 2006. Comparative peptide-binding studies of PABC domains from the E3 ubiquitin ligase HYD and poly(A)-binding protein: implications for HYD function. *J. Biol. Chem.* **281**: 14376–14382.

Lorenzen TJ, Anderson VL. 1993. Design of Experiments: A No-name Approach. Marcel Dekker: New York.

McDonnell JM. 2001. Surface plasmon resonance: towards an understanding of the mechanisms of biological molecular recognition. *Curr. Opin. Chem. Biol.* **5**: 572–577.

Moffett S, Mélançon D, De Crescenzo G, St-Pierre C, DesChenes F, Saragovi UH, Gold P, Cuello AC. 2007. Preparation and characterization of new anti-PSMA monoclonal antibodies with potential clinical uses. *Hybridoma* **26**: 363–372.

Montgomery DC. 2005. Design and Analysis of Experiments. John Wiley & Sons: New York.

Morton TA, Myszka DG. 1998. Kinetic analysis of macromolecular interactions using surface plasmon resonance biosensors. *Meth. Enzymol.* **295**: 268–294.

Myszka DG. 1997. Kinetic analysis of macromolecular interactions using surface plasmon resonance biosensors. *Curr. Opin. Biotechnol.* **8**: 50–57.

Myszka DG, Morton TA. 1998. CLAMP©: a biosensor kinetic analysis data program. *Trends Biochem. Sci.* **23**: 149–150.

Myszka DG, He X, Dembo M, Morton TA, Goldstein B. 1998. Extending the range of rate constants available from Biacore: interpreting mass transport-influenced binding data. *Biophys. J.* **75**: 583–594.

Ober RJ, Ward ES. 1999. The influence of signal noise on the accuracy of kinetic constants measured by surface plasmon resonance experiments. *Anal. Biochem.* **273**: 49–59.

O'Shannessy DJ, Winzor DJ. 1996. Interpretation of deviations from pseudo-first-order kinetic behavior in the characterization of ligand binding by biosensor technology. *Anal. Biochem.* **236**: 275–283.

Önell A, Andersson K. 2005. Kinetic determinations of molecular interactions using Biacore—minimum data requirements for efficient experimental design. *J. Mol. Recognit.* **18**: 307–317.

Pronzato L, Walter E. 1989. Experiment design in a bounded-error context: comparison with D-optimality. *Automatica* **25**: 383–391.

Rich RL, Myszka DG. 2000. Advances in surface plasmon resonance biosensor analysis. *Curr. Opin. Biotechnol.* **11**: 54–61.

Rich RL, Myszka DG. 2006. Survey of the year 2005 commercial optical biosensor literature. *J. Mol. Recognit.* **19**: 478–534.

Rich RL, Myszka DG. 2007. Higher-throughput, label-free, real-time molecular interaction analysis. *Anal. Biochem.* **361**: 1–6.

Rich RL, Cannon MJ, Jenkins J, Pandian P, Sundaram S, Magyar R, Brockman J, Lambert J, Myszka DG. 2008. Extracting kinetic rate constants from surface plasmon resonance array systems. *Anal. Biochem.* **373**: 112–120.

Sarrazin S, Bonnaffe D, Lubineau A, Lortat-Jacob H. 2005. Heparan sulfate mimicry: a synthetic glycoconjugate that recognizes the heparin binding domain of interferon-gamma inhibits the cytokine activity. *J. Biol. Chem.* **280**: 37558–37564.

Svitel J, Balbo A, Mariuzza RA, Gonzales NR, Schuck P. 2003. Combined affinity and rate constant distributions of analyte or ligand populations from experimental surface binding and kinetics and equilibria. *Biophys. J.* **84**: 4062–4077.

Wiley HS, Shavartsman SY, Lauffenburger DA. 2003. Computational modeling of the EGF-receptor system: a paradigm for systems biology. *Trends Cell Biol.* **13**: 43–50.